

# Analyses of the melt cooling rate in the melt-spinning process

**B. Karpe, B. Kosec\*, M. Bizjak**

Faculty of Natural Sciences and Engineering, University of Ljubljana,  
Aškerčeva cesta 12, Ljubljana, Slovenia

\* Corresponding e-mail address: borut.kosec@omm.ntf.uni-lj.si

Received 19.02.2012; published in revised form 01.04.2012

## Manufacturing and processing

### ABSTRACT

**Purpose:** Rapid solidification (RS) of metallic melts is important for the development of the advance metallic materials, because enables the production of new alloys with superior properties according to conventionally treated alloys. In practice it turned out, that single roll melt spinning process has one of the highest melt cooling rates among all continuous casting processes. But, because very short solidification time and movement of the melt and substrate, melt cooling rate is very difficult to measure with confidence. Primary goal of our work was to determine the limits of cooling rate over the ribbon thickness and to outline, which property or typical feature of the process has the greatest influence on cooling rate of the melt.

**Design/methodology/approach:** On the basis of developed mathematical model, a computer program was made and used for melt cooling rate calculation in the melt-spinning process.

**Findings:** The calculations show that distance from the contact surface in relation to the thermal properties of the melt, chilling wheel material and contact resistance between metal melt and chilling wheel have the greatest influence on melt/ribbon cooling rate. In the case of continuous casting, significant "long term" surface temperature increase may take place, if the wheel is not internally cooled.

**Research limitations/implications:** Influence of the melt physical properties, chill wheel material, contact resistance and cooling mode of the chill wheel on melt cooling rate are outlined.

**Practical implications:** Practical limits of melt cooling rate over ribbon thickness are outlined and directions for the chill wheel cooling system design are indicated.

**Originality/value:** Comparison between cooling rates calculated at various thermal resistance assumptions of particular constituents is outlined. New method for determining contact resistance through variable heat transfer coefficient is introduced which takes into account physical properties of the casting material, process parameters and contact time/length between metal melt/ribbon and substrate and enables cooling rate prediction before the experiment execution. In the case of continuous casting, heat balance of the melt-spinning process is calculated and influence of the chill wheel cooling mode on cooling rate of metallic ribbon is analyzed.

**Keywords:** Modelling; Rapid solidification; Metallic materials; Heat transfer; Heat transfer coefficient

#### Reference to this paper should be given in the following way:

B. Karpe, B. Kosec, M. Bizjak, Analyses of the melt cooling rate in the melt-spinning process, Journal of Achievements in Materials and Manufacturing Engineering 51/2 (2012) 59-66.

## 1. Introduction

Rapid solidification (RS) of metallic melts is important for the development of the advance metallic materials, because

enables the production of new alloys with superior properties according to conventionally treated alloys [1-3]. What is the speed of solidification, which divides between classical procedures of casting and rapid solidification, is not exactly

specified. Differences in interpretation refer to the development of final microstructure, but the characteristic of all rapid solidification techniques is a final non-equilibrium state of the microstructure [4,5], which can be seen as: refined grains, extended solubility in metal matrix, quantitative and qualitative change of microstructural constituents, reduced micro segregation, etc.

In general, rapid solidification of melts could be achieved by two approaches:

- with high undercooling of the melt prior solidification, by reduction or even elimination of heterogeneous nucleation sites in so called containerless processes (atomization, droplet emulsion technique, drop tube technique, magnetic levitation, etc.),
- with rapid cooling to bypass heterogeneous nucleation kinetically (melt-spinning, splat quenching, remelting of surface layer, etc.) [6-8]

Single roll melt spinning (Figure 1) is one of the most commonly used processes for rapid solidification. Its major advantage is the possibility of continuous production of rapidly solidified material in the form of thin ribbons or foils, even on large industrial scale [9-11]. In this technique, a thin stream of melt is directed onto a circumferential surface of a rotating wheel, where so called melt puddle forms (Figure 2).

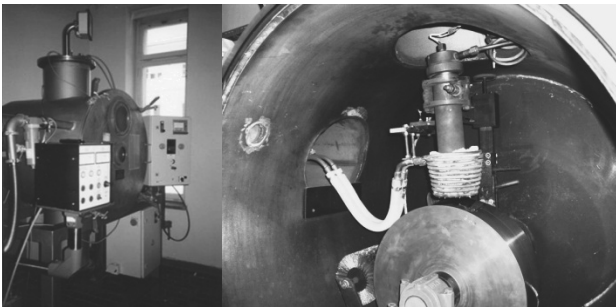


Fig. 1. Laboratory melt-spinning apparatus - Faculty of Natural Science and Engineering, University of Ljubljana (left), Componets assembly in the vacuum chamber (right)

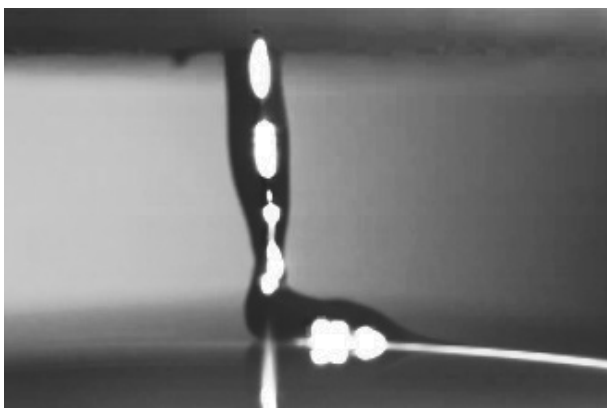


Fig. 2. Close-up speed frame camera snap shot of the melt puddle (tin casting) on the circumferential surface of the chill wheel, free jet melt-spinning [12]

Ribbon is then dragged out from the puddle by relative motion of the wheel. Microstructure of the ribbon can be completely crystalline, amorphous or combined and depends upon the contact resistance between the melt and substrate, latent heat of crystallization of casting material, heat transfer in the melt and the wheel, and nucleation and crystal growth characteristics of the particular casting material [13,14].

## 2. Heat transfer calculation

For calculation of temperature distribution inside the melt puddle and chill wheel, we used explicit finite difference method (FDM) with cylindrical coordinate system [15-17]. Thermal properties of the melt and wheel material ( $\lambda(T)$ ,  $c(T)$ ) are temperature dependent and calculated for each iteration step with linear interpolation from tabulated values of particular casting material. Density in solidification interval of the casting material is changing linearly, whereas density of the wheel material is approximated as constant. Because melt puddle is thin compare to its width and length we made an assumption of two-dimensional (2D) transient heat transfer. A schematic diagram of the idealized melt puddle geometry used in mathematical model is shown in Figure 2. Assuming 2D transient heat transfer with variable thermal properties and internal heat generation (latent heat of crystallization), general partial differential equation for the melt is reduced to:

$$\frac{1}{r} \cdot (\lambda \cdot \frac{\partial T}{\partial r}) + \frac{\partial}{\partial r} \cdot (\lambda \cdot \frac{\partial T}{\partial r}) + \frac{1}{r^2} \cdot \frac{\partial}{\partial \varphi} \cdot (\lambda \cdot \frac{\partial T}{\partial \varphi}) + q''' = \rho \cdot c \cdot \frac{\partial T}{\partial t} \quad (1)$$

And for chill wheel, where no latent heat is released:

$$\frac{1}{r} \cdot (\lambda \cdot \frac{\partial T}{\partial r}) + \frac{\partial}{\partial r} \cdot (\lambda \cdot \frac{\partial T}{\partial r}) + \frac{1}{r^2} \cdot \frac{\partial}{\partial \varphi} \cdot (\lambda \cdot \frac{\partial T}{\partial \varphi}) = \rho \cdot c \cdot \frac{\partial T}{\partial t} \quad (2)$$

where  $r$ ,  $\varphi$  represent spatial coordinates in cylindrical coordinate system [m; rad ],  $T$  temperature [ K ],  $\rho$  density [ $\text{kgm}^{-3}$ ],  $\lambda$  thermal conductivity [ $\text{Wm}^{-1}\text{K}^{-1}$ ],  $c$  specific heat of the melt or chill wheel material [ $\text{Jkg}^{-1}\text{K}^{-1}$ ], and  $q'''$  volumetric heat generation rate [ $\text{Wm}^{-3}$ ].

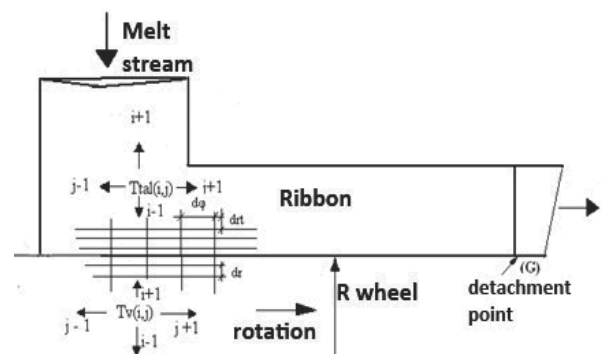


Fig. 3. Idealized geometry of the melt puddle used in mathematical model

Ribbon thickness is assumed to be proportional to circumferential velocity of the chill wheel ( $u_w^{-1}$ ) and the pressure in the crucible ( $p^{0.5}$ ), as predicted by continuity and Bernoulli equations. Temperature of the melt in the puddle direct under the impinging jet stays equal to casting temperature, because strong turbulences in that region. To ascertain the influence of the casting material thermal properties, chill wheel material, inner and external cooling of the chilling wheel, and contact resistance on cooling rate of the ribbon, comparison between calculated cooling rates at various assumptions was made: ideal isothermal wheel versus copper wheel, influence of various contact resistance, and influence of solidified ribbon thickness [18].

### 3. Results and discussion

Figure 4 represents calculated cooling curves of contact and free surface of cast ribbons in the case of an assumption of ideal isothermal cooling wheel and Figure 5 calculated cooling curves as a function of the distance from the contact surface.

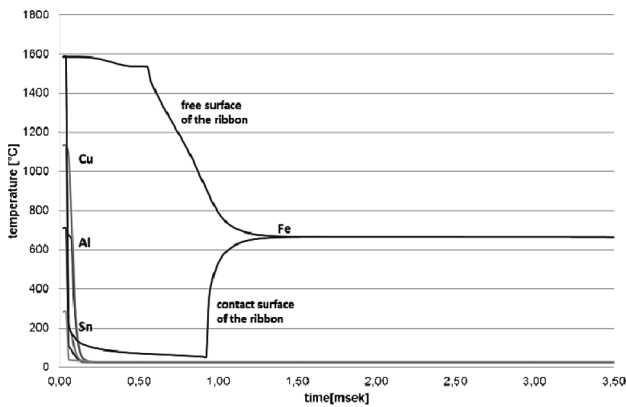


Fig. 4. Calculated cooling curves of free and contact surface of ribbons under assumption of ideal isothermal wheel

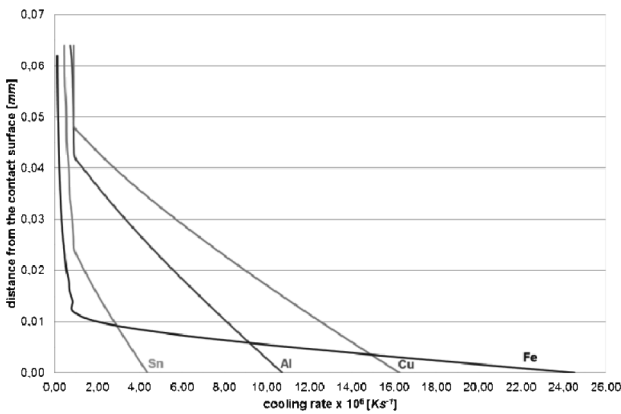


Fig. 5. Cooling rate as a function of a distance from the contact surface (Ideal isothermal wheel, ideal contact)

Calculations under assumption of ideal isothermal wheel indicate that 60  $\mu\text{m}$  thick ribbon would cool down to chill wheel temperature in an instant of time for most of the cast materials. The only exception is iron, as an example of material with high volumetric latent heat of crystallization, high melting point and relatively low thermal conductivity, where cooling rate of the 60  $\mu\text{m}$  thick ribbon free surface is much lower ( $\approx 10^5$ ) than cooling rate of the contact surface ( $\approx 2.5 \cdot 10^7$ ). Since in this calculation only takes into account the physical properties of the melt, we can conclude, that thermal properties of the melt itself, have significant influence on cooling rate across the transverse cross-section of the cast ribbon. Higher is the volumetric heat of crystallization of casting material ( $\Delta H_{\text{Fe}} > \Delta H_{\text{Cu}} > \Delta H_{\text{Al}} > \Delta H_{\text{Sn}}$ ), steeper will be melt cooling rate decrease, as a function of a distance from contact surface. When a layer of melt of a certain thickness solidifies, represent the only heat resistor and therefore the cooling rate in the remaining melt depends mainly on the thermal conductivity ( $\lambda_{\text{Cu}} > \lambda_{\text{Al}} > \lambda_{\text{Sn}} > \lambda_{\text{Fe}}$ ) of this solidified layer.

The next stage in calculations of heat transfer from the melt is to take into account real wheel material (copper) with finite thermal diffusivity (Figure 6). If we compare the calculation results to the results under assumption of ideal isothermal wheel, for all materials significantly longer solidification time, lower melt cooling rate over entire transverse cross section of a ribbon (Figure 7), and higher final temperature of the ribbon after detachment from the circumferential surface of the wheel is observed, although ribbon is only 60  $\mu\text{m}$  thick.

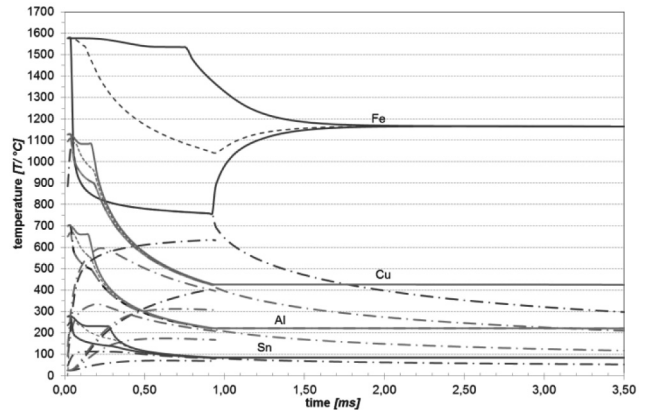


Fig. 6. Calculated cooling curves of contact and free ribbon surface cast on copper wheel. Hatched curves represent heating rate of copper wheel surface and 0.1 mm or 0.3 mm beneath the surface (thickness of cast ribbons 60  $\mu\text{m}$ , contact time 0.923 ms, ideal contact)

Decreased cooling rate of the melt and increased wheel surface temperature results from a fact that a high heat transfer takes place over short period of time. In spite of the high thermal diffusivity of copper, energy has no time to diffuse much into the wheel, and the surface of the wheel will heat up significantly. Consequently, because smaller temperature difference between the melt and the surface of the wheel, heat transfer rate and thus cooling rate of the remaining melt will also be reduced. Assumption of ideal isothermal wheel is not physically realistic,

because real materials can't absorb so much energy without heating up significantly.

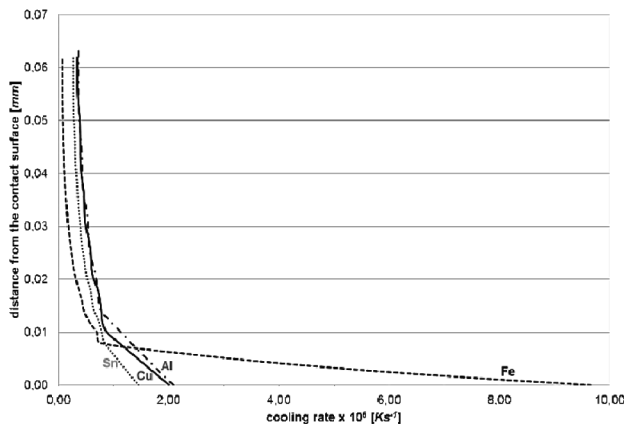


Fig. 7. Cooling rate as a function of a distance from the contact surface (Copper wheel, ideal contact)

Among thermal properties of the melt, volumetric heat of crystallization have major influence on melt cooling rate across the transverse cross-section of the cast ribbon. Figure 8 represent contact and free surface cooling curves of Al ribbon in dependence of the amount of the released crystallization heat. If we assume 50% lower crystallization heat, solidification time for free surface of 60 μm thick ribbon will decrease for 30%, and when amorphous solidification is presumed, 50% shorter is the time of solidification.

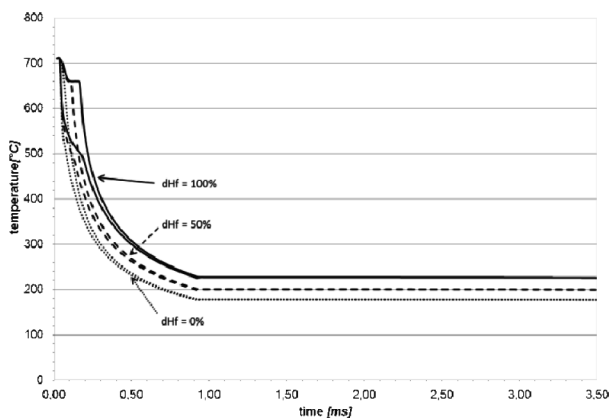


Fig. 8. Hypothetical calculated cooling curves of free and contact surface of Al ribbon as a function of different assumptions of latent heat of crystallization (ribbon thickness 60 μm, contact time 0.923 msec, ideal contact)

In situations where a detailed description of thermal physics is very complicated, such as in melt-spinning process, combined

modes of heat exchange are usually taken in to account with the overall heat transfer coefficient ( $\alpha$ ), which includes conduction and radiation of heat, as well as any convective effects. Ideal contact between the melt and wheel surface is not physically realistic, because there are no metallic atomic bonds between atoms of the melt and atoms of the surface of the wheel. By applying different values of heat transfer coefficient into calculations of heat transfer between melt and copper wheel surface, influence of contact resistance on cooling rate (Figure 9) could be estimated. In comparison to ideal contact (Figures 6, 7), cooling rate of the ribbon and cooling rate as a function of a distance from the contact surface (Figure 9) are relatively much lower when some contact resistance is considered, although the contact resistance value is very low ( $10^{-6} \text{ (m}^2\cdot\text{K)/W}$ ). Value for constant contact resistance for aluminum was obtained with subsequent microstructure analyses and reported by other authors [19]. Integral method calculation of the heat transfer coefficient gives the most logical results for entire duration of the contact. Calculated solidification time is practically the same to those obtained by overall (constant) heat transfer coefficient, but final temperature of the ribbon at the detachment point is much greater, especially for longer contact time. Constant contact resistance approximation ( $10^{-6} \text{ (m}^2\cdot\text{K)/W}$ ) for longer contact time predicts even lower ribbon temperature then ideal contact calculation, which is physically unlikely. The local heat transfer coefficient  $\alpha(x)$  is calculated with the integral method for liquid metals flow over flat plate [18,20]. The equation for local heat transfer coefficient  $\alpha(x)$  calculation, included in the numerical scheme is:

$$\alpha(x) = \frac{3 \cdot \lambda}{2 \cdot \sqrt{8}} \cdot \sqrt{\frac{u_w}{a \cdot x}} \quad (3)$$

where  $u_w$  represent circumferential velocity of the wheel [ $\text{ms}^{-1}$ ],  $\lambda$  thermal conductivity of the casting material [ $\text{Wm}^{-1}\text{K}^{-1}$ ],  $a$  temperature diffusivity of the casting material [ $\text{m}^2\text{s}^{-1}$ ], and  $x$  distance from the initial contact point to the actual calculation point [m].

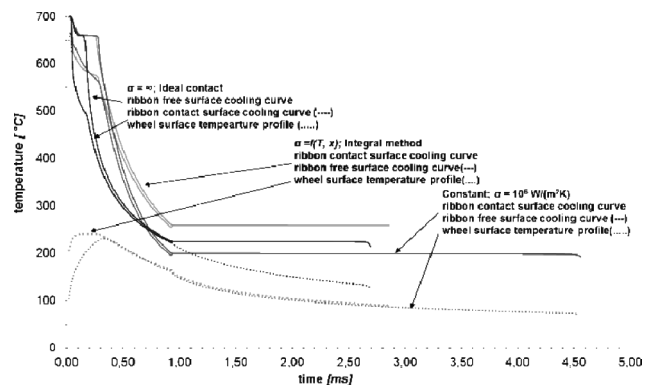


Fig. 9. Cooling curves of free and contact surface of Al ribbon and contact surface of the copper wheel as a function of different contact resistance (ribbon thickness 60 μm, contact time 0.923 msec)

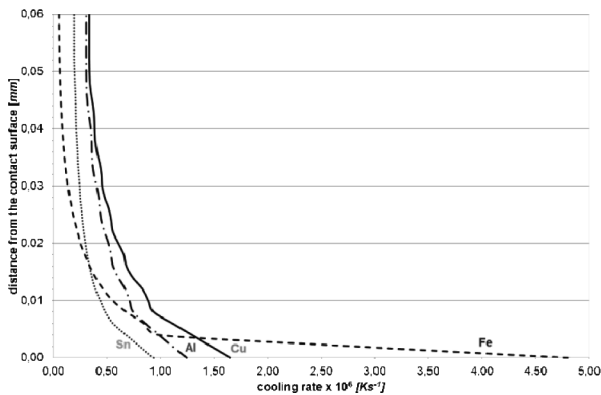


Fig. 10. Cooling rate as a function of a distance from the contact surface for different cast materials ( $\alpha(x)$  = integral method)

Figure 11 shows calculated temperature profiles in steel or copper wheel, when aluminum melt is cast. As we can see, surface temperature will increase significantly, especially for a wheel of low thermal diffusivity. Because limited thermal diffusion in the wheel, the energy can penetrate only a short distance in the wheel, which results in a higher temperature at the wheel surface. The magnitude of temperature increase depends on the wheel material. For steel wheel, which has much lower thermal diffusivity than copper, an increase of surface temperature is over 400°C, and heat penetration depth about 0.5 mm. On contrary, copper wheel surface temperature increase is about 200°C and penetration depth twice as much.

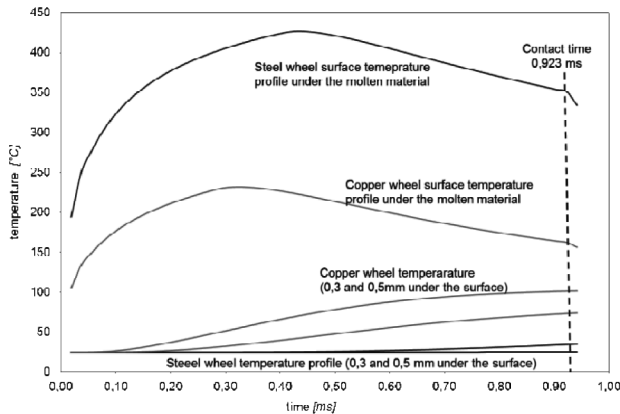


Fig. 11. Wheel temperature increase as a function of contact time and wheel material (Al casting)

Irrespective of contact resistance approximation, when aluminum melt is cast, the wheel surface temperature after reaching its maximum decrease, although it is in contact with hotter ribbon. This seems unlikely, but if we consider the wheel as a whole, its enthalpy is constantly rising, since temperature more than 0.3 mm under the surface is increasing the entire contact time. Namely, conduction heat transfer rate in the wheel is faster than the heat transfer rate across ribbon/wheel interface and through solidified ribbon.

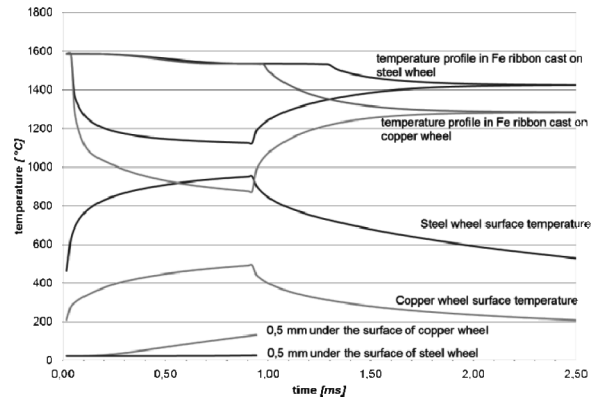


Fig. 12. Cooling curves for Fe ribbon and temperature profile in the wheel as a function of chill wheel material (ribbon thickness 60  $\mu\text{m}$ , contact time 0.923 msec,  $\alpha = \text{const. } 10^6 \text{ W/m}^2\text{K}$ )

When materials with higher melting point are cast, surface temperature will increase much higher (Figure 12). Obviously, such a large deviation in surface temperature should not be neglected in calculation of cooling and solidification rate of the melt. Importance of wheel material selection is evident. Pure deoxidized copper has the highest thermal diffusivity between all commercially useful materials and therefore is the best choice for the wheel material. In the case of the need for increased strength, oxide dispersive strengthened (ODS) copper alloys are best solution. When thicker ribbons are cast or materials with lower thermal conductivity, thermal resistance in already solidified region of the ribbon becomes the limiting factor of the heat transfer. High cooling and solidifying rates, through entire cross section of the ribbon can be achieved only when very thin ( $< 30\mu\text{m}$ ) ribbons are cast (Figures 13, 14).

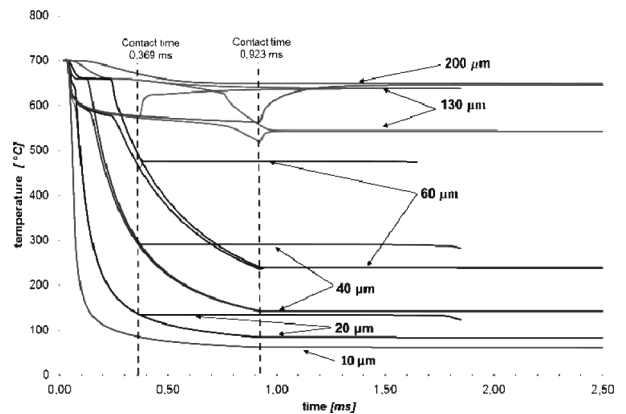


Fig. 13. Cooling curves of aluminum ribbon as a function of its thickness ( $\alpha(x)$  = integral method)

During continuous casting process, significant “long term” surface temperature increase may take place, if the wheel is not externally or internally cooled. In calculations discussed above, we have assumed that the wheel surface is at room temperature at the beginning of the contact.



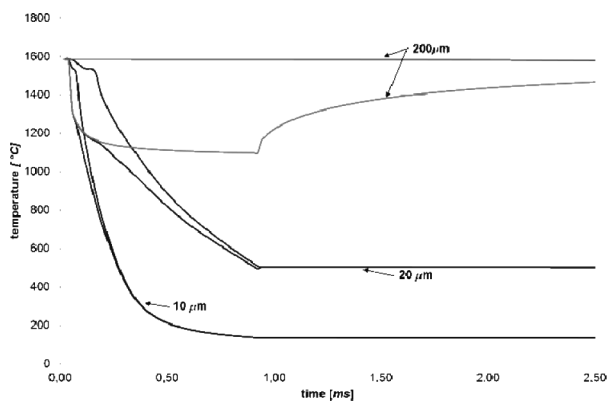


Fig. 14. Cooling curve of iron ribbon as a function of its thickness ( $\alpha(x)$  = integral method)

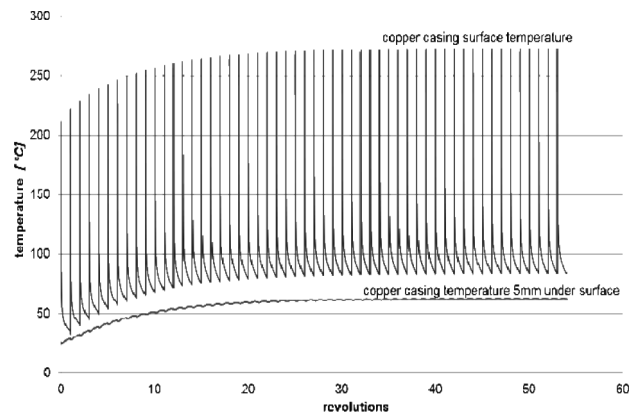
For first ten to hundred revolutions surface temperature increase may indeed not be significant, but when continuous casting is performed, especially when materials with high melting point are cast, surface temperature of the wheel can increase in such an extent, that formation of the ribbon will be disturbed, because of decreased cooling and solidifying rate in the melt puddle.

Figure 15 shows calculated temperature profiles in inner water cooled wheel ( $R_w = 0.2$  m) with different casing thickness. From the outside, wheel is convectively cooled with surrounding atmosphere, and from the inside with water stream. For simplicity of the mathematical model, convective heat transfer coefficients are taken as constants ( $\alpha_{\text{water}} = 5000$  W/(m<sup>2</sup>·K) and  $\alpha_{\text{air}} = 50$  W/(m<sup>2</sup>·K)) and represent average values, calculated from forced convection correlation equations. No radiation from the crucible is taking into account. To ascertain influence of external cooling, we also make an assumption of exaggerated value for convective heat transfer coefficient ( $\alpha_{\text{air}} = 1000$  W/(m<sup>2</sup>·K)).

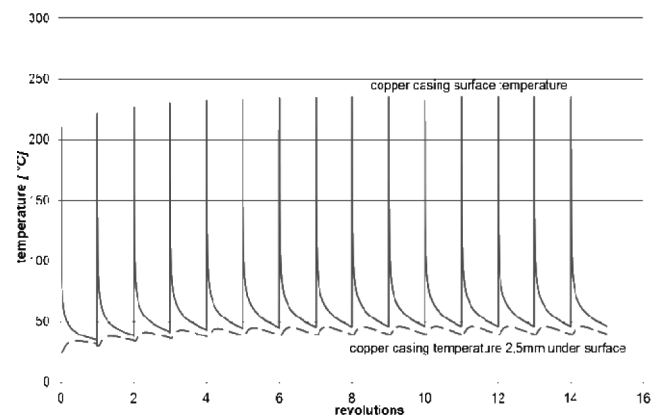
Each saw tooth spike corresponds to the temperature of the wheel surface being underneath the puddle. As we can see, internally water cooled wheel will reach the periodic steady state after few revolutions. Conducting of heat into the wheel and cooling of the inner casing surface with water stream is much faster than external convective cooling with surrounding atmosphere. If we reduce wheel casing thickness up to 2 mm, internal water cooling will be more effective, and wheel surface temperature that melt will effectively “feel” at the beginning of the next pass of the wheel under the puddle, will be practically the same as at the first revolution (Figure 15c), even if high melting temperature materials are cast.

But if we reduce wheel casing even further, beneath the heat penetration depth under the melt puddle, convective heat resistance on the inner side (wheel - water interface) becomes significant (Figure 16). Even if we assume heat transfer coefficient value on inner side of a casing as high as 100000 W/(m<sup>2</sup>·K), which can be reached only with high pressure impingement water jets [21], heat removal from the melt will still be slower as in the case of full or internally water cooled wheel with 10 mm thick casing (Figure 15a). Reducing the thickness of the wheel casing is unsuitable, from rapid solidification and from steadiness point of view.

a) 10 mm thick casing



b) 5 mm thick casing



c) 2 mm thick casing

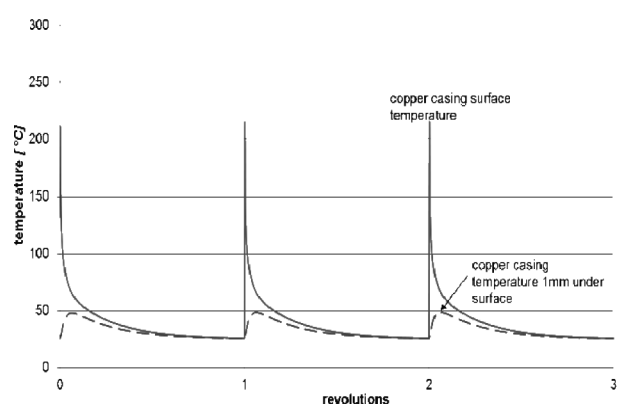


Fig. 15. Surface temperature of the internally water cooled wheel as a function of copper casing thickness a) 10 mm b) 5 mm c) 2 mm (aluminum casting, wheel radius 0.2 m)

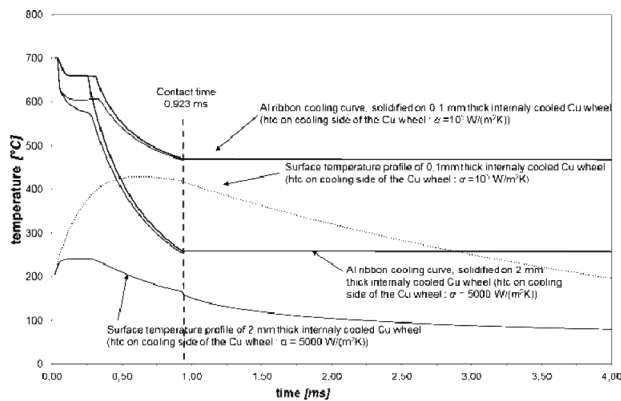


Fig. 16. Temperature profile in aluminium ribbon and surface temperature of the internally water cooled wheel as a function of copper casing thickness (0.1 mm and 2 mm thick casing)

In the case of external cooling with gas, “long term” surface temperature increase is practically the same as in the case without external cooling, although we assume exaggerated value [20,22] ( $\alpha_{\text{air}} = 1000 \text{ W}/(\text{m}^2\cdot\text{K})$ ) for convective heat transfer coefficient. Namely, duration of one revolution of the wheel is so short that external gas convective cooling would have significant influence on the wheel surface temperature.

## 4. Conclusions

In our numerical model (FDM), new method for determining contact resistance through variable heat transfer coefficient is introduced which takes into account physical properties of the casting material, process parameters and contact time/length between metallic melt or metallic ribbon and substrate respectively, and enables cooling and solidifying rate prediction before the experiment execution. Comparison of the results, acquired at different assumptions of heat transfer resistances shows, that heat contact resistance between the melt and the chill wheel, and finite thermal diffusivity of the wheel material have great influence on cooling rate of the ribbon and must not be neglected in heat transfer calculations. The fact that the wheel surface temperature is increasing significantly under the melt puddle, selection of the wheel material is not trivial. Because copper has the highest thermal diffusivity between all commercially useful materials, we propose deoxidized copper for a wheel material, and in the case of the need for increased strength, oxide dispersive strengthened (ODS) copper alloys.

For continuous casting, internally cooled wheel is preferable, but only in the case, when wheel casing thickness is correctly selected. When too thick casing is applied, water cooling will not have adequate influence on wheel surface temperature increase. When the casing of the wheel is too thin, thermal resistance on the cooling side becomes the limiting factor, which reduces the heat transfer from the melt and consequently its cooling and solidifying rate.

## Acknowledgements

The authors want to thank professor Ladislav Kosec (University of Ljubljana) for mentorship at study of rapid solidification and development of advanced shape memory materials, professor Mirko Gojić (University of Zagreb) for scientific cooperation at synthesis and characterization of rapidly solidified alloys, and professor Mirko Soković (University of Ljubljana) for technical informations and discussions.

## References

- [1] M. Bizjak, L. Kosec, A.C. Kneissl, B. Kosec, The characterisation of microstructural changes in rapidly solidified Al-Fe alloys through measurement of their electrical resistance, *International Journal of Materials Research* 99/1 (2008) 101-108.
- [2] L.A. Dobrzański, Technical and economical issues of materials selection, Silesian Technical University, Gliwice, 1997.
- [3] H.H. Libermann, Rapidly solidified alloys, Marcel Dekker, London, 1993.
- [4] M. Gojić, L. Vrsalović, S. Kožuh, A.C. Kneissl, I. Anžel, S. Gudić, B. Kosec, M. Kliškić, Electrochemical and microstructural study of Cu-Al-Ni shape memory alloy, *Journal of Alloys and Compounds* 509/41 (2011) 9782-9790.
- [5] G. Lojen, I. Anžel, A.C. Kneissl, E. Unterweger, B. Kosec, M. Bizjak, Microstructure of rapidly solidified Cu-Al-Ni shape memory alloy ribbons, *Journal of Materials Processing Technology* 162/163 (2005) 220-229.
- [6] D. Herlach, P. Galenko, A. Holland, D. Moritz, *Metastable solids from undercooled melts*, Pergamon Materials Series, London, 2006.
- [7] L.A. Dobrzański, M. Musztyfaga, Influence of cooling rates on properties of pre-alloyed PM materials, *Journal of Achievements in Materials and Manufacturing Engineering*, 37/1 (2009) 28-35.
- [8] L.A. Dobrzański, M. Musztyfaga, Effect of cooling rates on sinter-hardened steels, *Journal of Achievements in Materials and Manufacturing Engineering* 37/2 (2009) 630-638.
- [9] B. Kosec, Device for rapid solidifying of metal alloys, *Eurotech* 3 (2004) 32-33.
- [10] T. Haga, K. Inoue, H. Watari, Micro-forming of Al-Si foil, *Journal of Achievements in Materials and Manufacturing Engineering* 40/2 (2010) 115-122.
- [11] B. Karpe, B. Kosec, T. Kolenko, M. Bizjak, Heat transfer analyses of continuous casting by free jet meltspinning device, *Metallurgy* 50/1 (2011) 13-16.
- [12] B. Karpe, Determination of convective variables in melt-spinning process, Ph.D. Thesis, University of Ljubljana, Faculty of Natural Sciences and Engineering, Ljubljana, 2011.
- [13] L. Katgerman, F. Dom, Rapidly solidified aluminium alloys by meltspinning, *Materials and Engineering A* 375-377 (2004) 1212-1216.
- [14] L.E. Collins, Overview of rapid solidification technology, *Canadian Metallurgy Quarterly* 25/2 (1986) 59-71.

- [15] W.S. Janna, Engineering Heat Transfer, CRC Press, Taylor and Francis Group, Boca Raton, 2009.
- [16] J.K. Carpenter, P.H. Steen, On the heat transfer to the wheel in planar - flow melt spinning, Metallurgical Transactions B, 21/2 (1990) 279-283.
- [17] T.J. Praisner, J.S. Chen, A. Tseng, An experimental study of process behavior in planar flow melt spinning, Metallurgical Transactions B 26 (1995) 1199-1208.
- [18] B. Karpe, B. Kosec, M. Bizjak, Modeling of heat transfer in the cooling wheel in the melt-spinning process, Journal of Achievements in Materials and Manufacturing Engineering 46/1 (2011) 88-94.
- [19] G.X. Wang, E.F. Matthys, Modeling of rapid solidification by melt spinning: effect of heat transfer in the cooling substrate, Material Science and Engineering A 136 (1991) 85-97.
- [20] M.N. Özsisik, Heat transfer, A basic approach, McGraw-Hill, London, 1985.
- [21] M. Ciofalo, I. Di Piazza, V. Brucatto, Investigation of the cooling of hot walls by liquid water sprays, International Journal of Heat and Mass Transfer 42 (1999) 1157-1175.
- [22] D.M. Stefanescu, Science and Engineering of casting solidification, Kluwen Academic/Plenum Publishers, Kluwen, 2005.